Journal of Nuclear Medicine, published on May 22, 2020 as doi:10.2967/jnumed.120.244509

^{64}Cu-DOTATATE PET in Patients with Neuroendocrine Neoplasms: Prospective, Head-to-Head Comparison of Imaging at 1 Hour and 3 Hours Post-Injection

Mathias Loft[1,2], Esben A Carlsen[1,2], Camilla B Johnbeck[1,2], Helle H Johannesen[1,2], Tina Binderup[1,2], Andreas Pfeifer[1,2], Jann Mortensen[1,2], Peter Oturai[1,2], Annika Loft[1,2], Anne K Berthelsen[1,2], Seppo W Langer[2,3], Ulrich Knigge[2,4], Andreas Kjaer[1,2]*

[1]Dept. of Clinical Physiology, Nuclear Medicine & PET and Cluster for Molecular Imaging, Dept. of Biomedical Sciences, Rigshospitalet and University of Copenhagen, Denmark

[2]ENETS Neuroendocrine Tumor Center of Excellence, Rigshospitalet, Copenhagen, Denmark

[3]Dept. of Oncology, Rigshospitalet, Denmark

[4]Depts. of Clinical Endocrinology and Surgical Gastroenterology, Rigshospitalet, Denmark

* Correspondence to Prof. Andreas Kjaer, MD, PhD, DMSc, Dept. of Clinical Physiology, Nuclear Medicine & PET, KF-4011, Rigshospitalet, Blegdamsvej 9, DK-2100 Copenhagen, Denmark. ORCHID: https://orcid.org/0000-0002-2706-5547. E-mail: akjaer@sund.ku.dk

First author: Mathias Loft, MD, PhD-fellow, Dept. of Clinical Physiology, Nuclear Medicine & PET, KF-4011, Rigshospitalet, Blegdamsvej 9, DK-2100 Copenhagen, Denmark. ORCHID: https://orcid.org/0000-0003-3024-5706. E-mail: mloft@sund.ku.dk

Word count: 5216

Running title (max 40 characters) ^{64}Cu-DOTATATE PET after 1 hour & 3 hours

Financial support: This project received funding from the European Union's Horizon 2020 research and innovation programme under grant agreements no. 670261 (ERC Advanced Grant) and 668532 (Click-It), the Lundbeck Foundation, the Novo Nordisk Foundation, the Innovation Fund Denmark, the Danish Cancer Society, Arvid Nilsson Foundation, Svend Andersen Foundation, the Neye Foundation, the Research Foundation of Rigshospitalet, the Danish National Research Foundation (grant 126), the Research Council of the Capital Region of Denmark, the Danish Health Authority, the John and Birthe Meyer Foundation and Research Council for Independent Research.

ABSTRACT

^{64}Cu-DOTATATE PET/CT imaging 1 hour (h) post-injection (p.i.) is excellent for lesion detection in patients with neuroendocrine neoplasms (NEN). We hypothesized that the imaging time window can be extended up to 3h p.i. without significant differences in the number of lesions detected. **Methods** From a prospective study, we compared, on a head-to-head basis, sets of ^{64}Cu-DOTATATE PET/CT images from 35 patients with NEN scanned 1h and 3h p.i. of 200 MBq ^{64}Cu-DOTATATE. The number of lesions on both scans were counted and grouped according to organs or regions and compared with negative binomial regression. Discordant lesions (visible on the 1h or 3h p.i. ^{64}Cu-DOTATATE PET but not the other) were considered true if found on simultaneous CT or later MR, CT or somatostatin receptor imaging. We measured lesion maximal standardized uptake values (SUV_{max}), reference normal organ or tissue mean SUV (SUV_{mean}) and tumor-to-normal tissue ratios (TTN) calculated from SUV_{max}/ SUV_{mean}. **Results** We found 822 concordant lesions (visible on both the 1h and 3h p.i. ^{64}Cu-DOTATATE PET) and five discordant lesions of which four were considered true. One discordant case in one patient involved a discordant organ system (lymph node) detected on the 3h p.i. but not the 1h p.i. ^{64}Cu-DOTATATE PET that did not alter the patient's disease stage (stage IV) because the patient had 11 additional concordant liver lesions. We found no significant differences between the number of lesions detected on the 1h and 3h p.i. ^{64}Cu-DOTATATE PET. Throughout the 1-3 h p.i. imaging window, TTN (mean [95% confidence interval]) remained high in all key organs: Liver (1h p.i.: 12.6 [10.2; 14.9] , 3h p.i.: 11.0 [8.7; 13.4]), intestines (1h p.i.: 24.2 [14.9; 33.4], 3h p.i.: 28.2 [16.5; 40.0]), pancreas (1h p.i.: 42.4 [12.3; 72.5], 3h p.i.: 41.1 [8.7; 73.4]) and bone (1h p.i.: 103.0 [38.6; 167.4], 3h p.i.: 124.2 [57.1; 191.2]). **Conclusion** The imaging time window of ^{64}Cu-DOTATATE PET/CT of patients with NEN can be expanded from 1h p.i. to 1-3 hours p.i. without significant differences in the number of lesions detected.

Keywords

^{64}Cu-DOTATATE; Somatostatin receptor imaging; Standardized uptake values (SUV); PET/CT, Neuroendocrine neoplasms

INTRODUCTION

Neuroendocrine neoplasms (NEN) represent a heterogeneous class of diseases with large variability in aggressiveness and prognosis. NEN most frequently originates from the pancreas, the gastro-intestinal tract or the lung (*1*). A common feature of most NEN is the overexpression of somatostatin receptors (SSTR) (*2,3*) and SSTR-imaging with radioactively labeled SSTR-specific peptides plays an important role in the staging, follow-up and treatment guidance of patients with NEN (*4-7*).

We have previously demonstrated that SSTR-targeting positron emission tomography (PET) imaging 1 hour (1h) post injection (p.i.) of 200 MBq ^{64}Cu-DOTATATE is excellent in lesion detection in patients with NEN compared with other clinically available ^{68}Ga-based PET and ^{111}In-based single photon emission computed tomography (SPECT) SSTR-imaging modalities (*8,9*). Accordingly, ^{64}Cu-DOTATATE PET was introduced at Rigshospitalet, Copenhagen, Denmark as routine SSTR-imaging of patients with NEN in 2018.

^{64}Cu has a low maximal positron energy (0.653 MeV) resulting in a short mean positron range (0.6 mm) that leads to excellent image resolution (*10*). For comparison, the mean positron range of ^{68}Ga is 2.9 mm (*11*). In addition, ^{64}Cu has the advantage of a longer half-life than ^{68}Ga (12.7 hours vs. 68 min) that prolongs the post-synthesis usage time of ^{64}Cu-based tracers compared with ^{68}Ga-based tracers. This allows for central production of the tracer at a ^{64}Cu-cyclotrone site and the tracer can then be distributed to other non-production sites with sufficient activity left at time of injection. The shelf life of ^{64}Cu-DOTATATE is 24h (*12*) making it possible to prepare the tracer on one day and inject and image patients the following day.

The long ^{64}Cu half-life also makes it possible to perform imaging in a broader time window and up to several hours p.i. with sufficient count statistics on later scans. An obvious benefit of the flexibility in acquisition timing is the possibility to complete a scan of an already injected patient if delays occur such that the scan cannot be completed at the target time (1h p.i.). Initial analysis from our first-in-human study with ^{64}Cu-DOTATATE suggested that the imaging window could be extended up to at

least 3h p.i. without loss of image quality or tumor detection ability (*12*). However, the study included a relatively small number of patients and no formal quantitative analysis on the lesion numbers were performed.

The aim of the current study was therefore, on a head-to-head basis, to compare quantitatively ^{64}Cu-DOTATATE PET/CT scans for tumor lesion detection in patients with NEN scanned at 1h p.i. and 3h p.i. in a larger group of patients. We hypothesized that the imaging time window can be expanded from 1h p.i. to 3h p.i. without significant differences in the number of lesions detected.

MATERIALS AND METHODS

Patients and Study Design

The study was part of our previously published prospective study of patients with NEN scanned with ^{64}Cu-DOTATATE PET/CT at Rigshospitalet, Copenhagen, Denmark from 2009 to 2013 (*8*). In this study, the first 35 patients were ^{64}Cu-DOTATATE PET/CT scanned both at 1h and 3h p.i. and these 35 sets of scans were included in the current head-to-head analysis. Patients were characterized by gender, age, primary tumor location, tumor functional status, tumor grade and previous NEN-related treatments. All patients had signed informed consent prior to inclusion. The study was approved by the Regional Scientific Ethical Committee (reference no. H-D-2008-045).

Radiotracer Synthesis and Image Acquisition

^{64}Cu-DOTATATE production and PET/CT imaging have previously been described in detail (*8,12*). In brief, ^{64}Cu-DOTATATE was produced in-house and the injected activity was approximately 200 MBq. Subsequent whole-body PET imaging (from scull to mid-thigh) was performed at 1h and 3h p.i. The axial *x* transaxial field of view was 216 *x* 205 mm and the acquisition time 3 minutes per bed. All patients were PET-scanned on a Biograph 64 TruePoint PET/CT scanner (Siemens Medical

Solutions) and the PET data were reconstructed with the TrueX algorithm (Siemens Medical Solutions) using 3 iterations and 21 subsets and smoothed by a Gaussian filter (2 mm full-width-half-maximum). A diagnostic CT scan was acquired prior to the 1h p.i. PET scan using a 3-mm slice thickness, 120 kV, and quality reference of 225 mA modulated by the Care Dose 4D automatic exposure control system (Siemens Medical Solutions). Unless contraindicated, patients received 75 mL of iodine-containing contrast agent administered with an automatic infusion system (Optiray 300; Covidien) with scan delays of 60 s (flow rate, 1.5 mL/s) followed by an infusion of 100 ml NaCl (flow rate, 2.5 mL/s). The diagnostic CT scan was used for attenuation correction of the 1h p.i. PET scan. Prior to the subsequent 3h p.i. PET scan, a low-dose CT (20 mA, 140 kV) without contrast was acquired for attenuation correction.

Imaging Analysis

The 1h p.i. and 3h p.i. ^{64}Cu-DOTATATE PET/CT scans were reviewed side-by-side from June to August 2019 by the same SSTR-reader in cooperation with a radiologist blinded to the previous imaging analysis. All foci were identified on PET, and the CT was used mainly to confirm the anatomical location of the PET foci. Lesion sites were divided into organs or regions: liver, pancreas, intestines, lung/pleura, bones, lymph nodes, intra-abdominal carcinomatosis, and other (soft tissue, heart, stomach, adrenal and other less common regions) and all PET-positive lesions (defined as a clearly detectable lesion distinguishable from the surrounding tissue or organ) in each organ or region were counted. The concordance of the lesions on the 1h p.i. and 3h p.i. ^{64}Cu-DOTATATE PET scans was assessed for each organ or region. Discordant findings were followed up until October 2019 (up to 10 years follow up) using available MR, CT or SSTR-images to determine if the discordant finding was a true lesion. A discordant finding was considered true if the lesion had a positive CT correlate on the 1h p.i. or 3h p.i. ^{64}Cu-DOTATATE PET/CT or could be found on a later SSRT-imaging modality or other imaging methods on follow-up.

To establish a set of reference uptake values for the ^{64}Cu-DOTATATE PET in patients with NEN, we also quantified uptakes in lesions and normal organs and tissue on both the 1h p.i. and 3h p.i. ^{64}Cu-DOTATATE PET. Maximum standardized uptake values (SUV_{max}) of the "hottest" concordant lesion, if any, in each region or group was measured from a region of interest covering the entire lesion. Mean standardized uptake values (SUV_{mean}) of reference organs or tissues were measured from spherical region of interests on: a non-diseased area of the right liver lobe, the lung adjacent to the right hilus, the cauda and the uncinate process of the pancreas, spleen, intestines (ileum), the gluteal muscle and an area 5 cm below the trochanter of the right femur for bone reference. Reference values for the pituitary gland and the adrenal glands were measured with the SyngoVIA isocontur region of interest tool (default threshold of 40% of max) of a region of interest covering the entire organ. Tumor-to-normal-tissue ratios (TTN) for lesions in the liver, pancreas and lung were calculated by dividing the lesion SUV_{max} with the SUV_{mean} of the non-diseased area of the corresponding organ. Similarly, the femur SUV_{mean} was used for bone TTN, intestinal SUV_{mean} for intestinal and intra-abdominal carcinomatosis TTN, and gluteal muscle SUV_{mean} for lymph node TTN. All images were analyzed using SyngoVIA Version VB30A-HF04 (Siemens Medical Solutions).

Statistical Methods

Differences in the number of lesions between the 1h p.i. and 3h p.i. ^{64}Cu-DOTATATE PET were analyzed with negative binomial regression. The 1h p.i. and 3h p.i. ^{64}Cu-DOTATATE PET lesion SUV_{max}, reference organ and tissue SUV_{mean} and TTN are shown as mean with 95 percent confidence intervals (95% CI) and were analyzed with paired T-tests adjusted for multiple comparisons by Bonferroni corrections (*13*). Two-sided p-values less than 0.05 were considered statistically significant. All statistical analyses were performed using R statistical software (R Foundation for Statistical Computing, Vienna, Austria) version 3.6.1.

RESULTS

Patients and Imaging Characteristics

A total of 35 patients had 1h p.i. and 3h p.i. ^{64}Cu-DOTATATE PET/CT images available and were included in the analysis. Mean [minimum, maximum] injected dose of ^{64}Cu-DOTATATE was 205 [183, 232] MBq. Tracer uptake time was 52.9 [43, 80] min and 180.0 [167, 194] min for the 1h p.i. and 3h p.i. ^{64}Cu-DOTATATE PET, respectively. The characteristics of the patients are shown in Table 1.

Lesion Numbers

The 1h p.i. and 3h p.i. ^{64}Cu-DOTATATE PET showed excellent image quality with detection of the majority of the lesions on both scans. Figure 1 shows representative examples of patients with detectable lesions on both the 1h p.i. and 3h p.i. ^{64}Cu-DOTATATE PET/CT in different organs: liver lesions (Figure 1A), bone lesion (Figure 1B), lymph node lesion (Figure 1C) and pancreatic lesion (Figure 1D). Lesions divided into organs and regions are shown in Table 2. A total of 822 lesions (99.4 % of all lesions) were identified on both the 1h p.i. and 3h p.i. ^{64}Cu-DOTATATE PET (concordant lesions), while five lesions (0.6 % of all lesions) were identified on one of the PET scans, but not on the other (discordant lesions). No significant differences in the number of lesions per organ/region or in the total number of lesions were found. Table 3 shows discordant findings on a per patient basis. The five discordant lesions were detected in five different patients. In four of the cases, the discordant lesion was present on the 3h p.i. ^{64}Cu-DOTATATE PET but not on the 1h p.i. ^{64}Cu-DOTATATE PET. Two of the discordant lesions (patient 1: lymph node and patient 4: bone) had visible CT correlates on the ^{64}Cu-DOTATATE PET/CT and were thus considered true positive (Figures 2 and 3). Two additional discordant findings (patients 3 and 5: liver) were considered true positive since they could be identified on later ^{68}Ga-DOTATOC-PET (Figures 4 and 5). The remaining discordant lesion (patient 2: bone) was

considered false positive since the lesion could not be identified on later imaging modalities (Figure 6). One of the discordant lesions (patient 1: lymph node) resulted in the involvement of an additional organ system on the 3h p.i. ^{64}Cu-DOTATATE PET not detected on the 1h p.i. ^{64}Cu-DOTATATE PET. This patient had 11 additional concordant metastatic liver lesions.

Quantitative Image Analysis of Lesions and Reference Organs/Tissue Uptake

Lesion SUV_{max} divided into organs/regions are shown in Table 4 and SUV_{mean} of normal organs and tissues are shown in Table 5. Table 6 shows the TTN for the different lesions in patients with lesions and evaluable normal tissue in the corresponding region or organ.

DISCUSSION

In this prospective study of ^{64}Cu-DOTATATE in 35 patients with NEN we investigated the hypothesis that ^{64}Cu-DOTATATE PET may be performed from 1h to 3h p.i. without loss of the lesion detection ability compared with 1h p.i. imaging. Our main finding was that ^{64}Cu-DOTATATE can be used for PET imaging of patients with NEN from 1-3h p.i. with high TTN (lesion contrast) and a stable lesion detection rate without significant differences in the number of lesions detected. In comparison with the fixed 1h p.i. acquisition time of ^{68}Ga-labeled SSRT-PET tracers, the expansion of the acquisition time window of ^{64}Cu-DOTATATE PET is convenient in the daily clinical routine.

The high agreement in the number of lesions and organ systems detected on both the 1h p.i. and 3h p.i. ^{64}Cu-DOTATATE PET supports the rationale of expanding the imaging time window. The two additional true positive liver lesions found on the 3h p.i. ^{64}Cu-DOTATATE PET further suggests that in difficult cases with clinical suspicion of a small liver focus, it might be advantageous to perform late

phase ^{64}Cu-DOTATATE PET imaging at 3h p.i. if nothing is found on the 1h p.i. ^{64}Cu-DOTATATE PET. Of the five discordant lesions, only one case resulted in involvement of an additional organ system (patient 1: lymph node) on the 3h p.i. ^{64}Cu-DOTATATE PET not registered on the 1h p.i. ^{64}Cu-DOTATATE PET. Since the patient had 11 concordant metastatic liver lesions, the patient's disease stage would not have changed from stage IV as a consequence of the additional lymph node detected on the 3h p.i. ^{64}Cu-DOTATATE PET (*14*). However, the finding of an additional extra-hepatic lesion in one patient with liver-only lesions could potentially have an impact on the clinical management. In the remaining four cases, the discordant findings involved lesions in already concordant organ systems.

The relatively short follow-up between the ^{64}Cu-DOTATATE PET/CT and the latest available CT for patient 2 (8 months) may explain why the discordant bone lesion could not be confirmed. For ^{64}Cu-DOTATATE (*8,9*), ^{68}Ga-DOTATOC (*15*) and ^{68}Ga-DOTATATE (*16*), bone lesions are detected on PET several months to years prior to detection on CT in some cases. Alternatively, the finding may represent an artifact on the 1h p.i. ^{64}Cu-DOTATATE PET. Importantly, the patient also had several concordant bone lesions. The clinical consequences of the false positive findings are very limited.

It has been questioned whether the ^{64}Cu-DOTATATE liver uptake could be a challenge for detection of liver lesions. Although a numerical increase in the mean liver SUV_{mean} on the 3h p.i. compared with the 1h p.i. ^{64}Cu-DOTATATE PET was seen, the median liver SUV_{mean} for ^{64}Cu-DOTATATE in our study (1h p.i. 3.86 and 3h p.i. 5.52) was still lower at both time points compared to what has been reported for another ^{64}Cu-labeled SSTR-PET tracer ^{64}Cu-SARTATE (1h p.i. 7.10 and 4h p.i. 5.90) (*17*). The mean liver SUV_{mean} at both 1h p.i. and 3h p.i. for ^{64}Cu-DOTATATE was also within the range or lower than that reported for ^{68}Ga-DOTATATE at 1h p.i.: 4.5 (*18*) to 7.2 (*19*). In addition, because the liver lesion SUV_{max} also increased from the 1h p.i. to 3h p.i. ^{64}Cu-DOTATATE, the mean liver TTN remained high and almost unchanged from 1h p.i. to 3h p.i. (12.6 vs 11.0). Importantly, moreover the liver lesion detection ability at 3h p.i. was not affected as two additional true liver lesions were identified on

the 3h p.i. ^{64}Cu-DOTATATE PET. Although it could be discussed whether the use of two different CT scans for the attenuation correction for the 1h p.i. and 3h p.i. PET could have contributed to differences in the quantification at the two time points, we find this unlikely to have been of any clinical relevance (*20,21*).

It could be speculated whether differences in liver background and liver lesion uptake between the 1h p.i. and 3h p.i. ^{64}Cu-DOTATATE PET should be taken into consideration when ^{64}Cu-DOTATATE PET is used for selection of patients for peptide receptor radionuclide therapy (PRRT). However, apart from a single bone lesion, all lesions in all the patients were above liver background uptake both at 1h p.i. and 3h p.i.. Therefore, if the a modified Krenning scale had been applied, the conclusions would be similar whether based on 1h p.i. or 3h p.i. ^{64}Cu-DOTATATE PET. However, if more quantitative cut-offs will be established in the future for guiding PRRT, they are likely to be both PET tracer and scan time specific.

The high TTNs measured on both the 1h p.i. to 3h p.i. ^{64}Cu-DOTATATE PET throughout the different organs and regions suggest that the tumor delineation from the surroundings remains sufficient in the 1-3h p.i. time window. Combined with the high concordance in the number of lesions detected on both the 1h p.i. and 3h p.i. ^{64}Cu-DOTATATE PET, this observation supports the conclusion that no clinically relevant loss in image information occurs within the 1-3h p.i. imaging window.

CONCLUSION

^{64}Cu-DOTATATE PET/CT has excellent performance from 1-3h p.i. for imaging patients with NEN without significant differences in the number of lesions detected. The maintained lesion detection rate and high contrast from 1-3h p.i., combined with the shelf life of 24h, adds to the convenience and flexibility of using ^{64}Cu-DOTATATE PET for routine imaging of patients with NEN.

KEYPOINTS

QUESTIONS: Can the imaging time window for ^{64}Cu-DOTATATE PET be expanded from 1 hour post-injection (p.i.) to 1-3 hours p.i. in patients with neuroendocrine neoplasms (NEN)?

PERTINENT FINDINGS: ^{64}Cu-DOTATATE PET/CT imaging has excellent performance with high TTN and conserved lesion detection ability from 1-3 hours p.i. in patients with NEN.

IMPLICATIONS FOR PATIENT CARE: The imaging time window can be expanded from 1 hour p.i. to 1-3 hours p.i. which adds to the convenience and flexibility of using ^{64}Cu-DOTATATE PET for routine imaging in patients with NEN.

DISCLOSURE

Andreas Kjaer and Ulrich Knigge are inventors on patent/applications covering “PET tracer for imaging of neuroendocrine tumors”. The other authors have no potential conflicts of interests relevant to this article.

ACKNOWLEDGEMENTS

We are grateful to the staff at the Department of Clinical Physiology, Nuclear Medicine, and PET for help with performing the PET/CT studies.

REFERENCES

1. Yao JC, Hassan M, Phan A, et al. One hundred years after "carcinoid": epidemiology of and prognostic factors for neuroendocrine tumors in 35,825 cases in the United States. *J Clin Oncol.* 2008;26:3063-3072.

2. Papotti M, Croce S, Macri L, et al. Correlative immunohistochemical and reverse transcriptase polymerase chain reaction analysis of somatostatin receptor type 2 in neuroendocrine tumors of the lung. *Diagn Mol Pathol.* 2000;9:47-57.

3. Oberg KE, Reubi JC, Kwekkeboom DJ, Krenning EP. Role of somatostatins in gastroenteropancreatic neuroendocrine tumor development and therapy. *Gastroenterology.* 2010;139:742-753.

4. Sundin A, Arnold R, Baudin E, et al. ENETS consensus guidelines for the standards of care in neuroendocrine tumors: radiological, nuclear medicine & hybrid imaging. *Neuroendocrinology.* 2017;105:212-244.

5. Strosberg JR, Halfdanarson TR, Bellizzi AM, et al. The North American neuroendocrine tumor society xonsensus guidelines for surveillance and medical management of midgut neuroendocrine tumors. *Pancreas.* 2017;46:707-714.

6. Janson ET, Sorbye H, Welin S, et al. Nordic guidelines 2014 for diagnosis and treatment of gastroenteropancreatic neuroendocrine neoplasms. *Acta Oncol.* 2014;53:1284-1297.

7. Bozkurt MF, Virgolini I, Balogova S, et al. Guideline for PET/CT imaging of neuroendocrine neoplasms with ^{68}Ga-DOTA-conjugated somatostatin receptor targeting peptides and ^{18}F-DOPA. *Eur J Nucl Med Mol Imaging.* 2017;44:1588-1601.

8. Pfeifer A, Knigge U, Binderup T, et al. ^{64}Cu-DOTATATE PET for neuroendocrine tumors: a prospective head-to-head comparison with ^{111}In-DTPA-Octreotide in 112 patients. *J Nucl Med.* 2015;56:847-854.

9. Johnbeck CB, Knigge U, Loft A, et al. Head-to-head comparison of ^{64}Cu-DOTATATE and ^{68}Ga-DOTATOC PET/CT: A prospective study of 59 patients with neuroendocrine tumors. *J Nucl Med.* 2017;58:451-457.

10. Jodal L, Le Loirec C, Champion C. Positron range in PET imaging: non-conventional isotopes. *Phys Med Biol.* 2014;59:7419-7434.

11. Bailey DL, Maisey MN, Townsend DW, Valk PE. *Positron emission tomography.* Vol 2: London, Springer; 2005:22.

12. Pfeifer A, Knigge U, Mortensen J, et al. Clinical PET of neuroendocrine tumors using ^{64}Cu-DOTATATE: first-in-humans study. *J Nucl Med.* 2012;53:1207-1215.

13. Bland JM, Altman DG. Multiple significance tests: the Bonferroni method. *BMJ.* 1995;310:170.

14. Rindi G, Kloppel G, Alhman H, et al. TNM staging of foregut (neuro)endocrine tumors: a consensus proposal including a grading system. *Virchows Arch.* 2006;449:395-401.

15. Putzer D, Gabriel M, Henninger B, et al. Bone metastases in patients with neuroendocrine tumor: ^{68}Ga-DOTA-Tyr3-octreotide PET in comparison to CT and bone scintigraphy. *J Nucl Med.* 2009;50:1214-1221.

16. Albanus DR, Apitzsch J, Erdem Z, et al. Clinical value of ^{68}Ga-DOTATATE-PET/CT compared to stand-alone contrast enhanced CT for the detection of extra-hepatic metastases in patients with neuroendocrine tumours (NET). *Eur J Radiol.* 2015;84:1866-1872.

17. Hicks RJ, Jackson P, Kong G, et al. ^{64}Cu-SARTATE PET imaging of patients with neuroendocrine tumors demonstrates high tumor uptake and retention, potentially allowing prospective dosimetry for peptide receptor radionuclide therapy. *J Nucl Med.* 2019;60:777-785.

18. Kunikowska J, Krolicki L, Pawlak D, Zerizer I, Mikolajczak R. Semiquantitative analysis and characterization of physiological biodistribution of ^{68}Ga-DOTA-TATE PET/CT. *Clin Nucl Med.* 2012;37:1052-1057.

19. Shastry M, Kayani I, Wild D, et al. Distribution pattern of ^{68}Ga-DOTATATE in disease-free patients. *Nucl Med Commun.* 2010;31:1025-1032.

20. ter Voert EE, van Laarhoven HW, Kok PJ, Oyen WJ, Visser EP, de Geus-Oei LF. Comparison of liver SUV using unenhanced CT versus contrast-enhanced CT for attenuation correction in ^{18}F-FDG PET/CT. *Nucl Med Commun.* 2014;35:472-477.

21. Yau Y-Y, Chan W-S, Tam Y-M, et al. Application of intravenous contrast in PET/CT: does it really introduce significant attenuation correction error? *J Nucl Med.* 2005;46:283-291.

FIGURE 1 Representative examples of lesions in the same patients scanned at 1h p.i. and 3h p.i. From left to right: CT, ^{64}Cu-DOTATATE PET, fused ^{64}Cu-DOTATATE PET/CT and maximum intensity projection (MIP) with corresponding SUV color bars below. For each example, the 1h p.i. ^{64}Cu-DOTATATE PET/CT is on top and the 3h p.i. ^{64}Cu-DOTATATE PET/CT in on the bottom. **A** Liver lesions, **B** bone lesion, **C** lymph node lesion, **D** pancreatic lesion. All lesions were identified on both the 1h p.i. and 3h p.i. ^{64}Cu-DOTATATE PET. Ant: anterior, Post: posterior, R: right, L: left, H: head, F: feet.

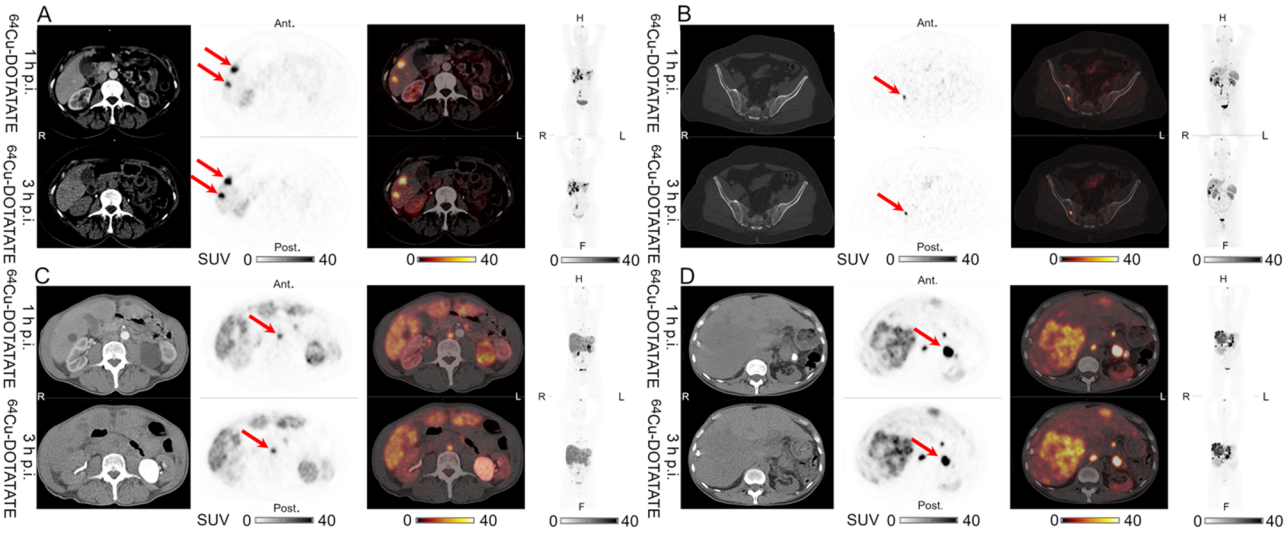

FIGURE 2 Patient 1: One additional lymph node lesion visible on 3h p.i. ^{64}Cu-DOTATATE PET (middle) but not 1h p.i. ^{64}Cu-DOTATATE PET (top) with visible CT correlate. The lymph node lesion was also visible on later 1h p.i. ^{64}Cu-DOTATATE-PET/CT with CT correlate performed 9 months after the initial scan (bottom). True positive. From left to right: CT, ^{64}Cu-DOTATATE PET, fused ^{64}Cu-DOTATATE PET/CT and MIP with corresponding SUV color bars below. Ant.: anterior, Post.: posterior, R: right, L: left, H: head, F: feet.

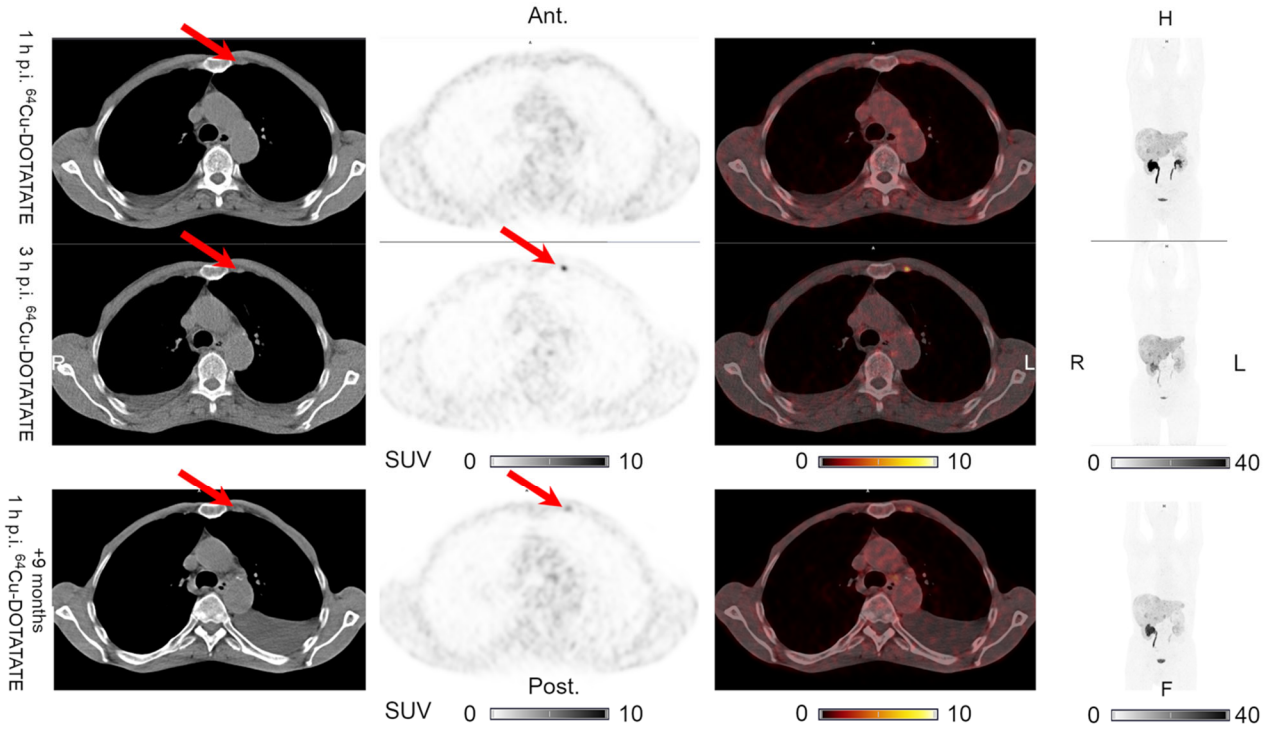

FIGURE 3 Patient 4: One additional bone lesion visible on 3h p.i. ^{64}Cu-DOTATATE-PET (bottom) but not 1h p.i. ^{64}Cu-DOTATATE PET (top) with visible CT correlate. True positive. No later SSTR-PET available. From left to right: CT, ^{64}Cu-DOTATATE PET, fused ^{64}Cu-DOTATATE PET/CT and MIP with corresponding SUV color bar below. A: anterior, P: posterior, R: right, L: left, H: head, F: feet.

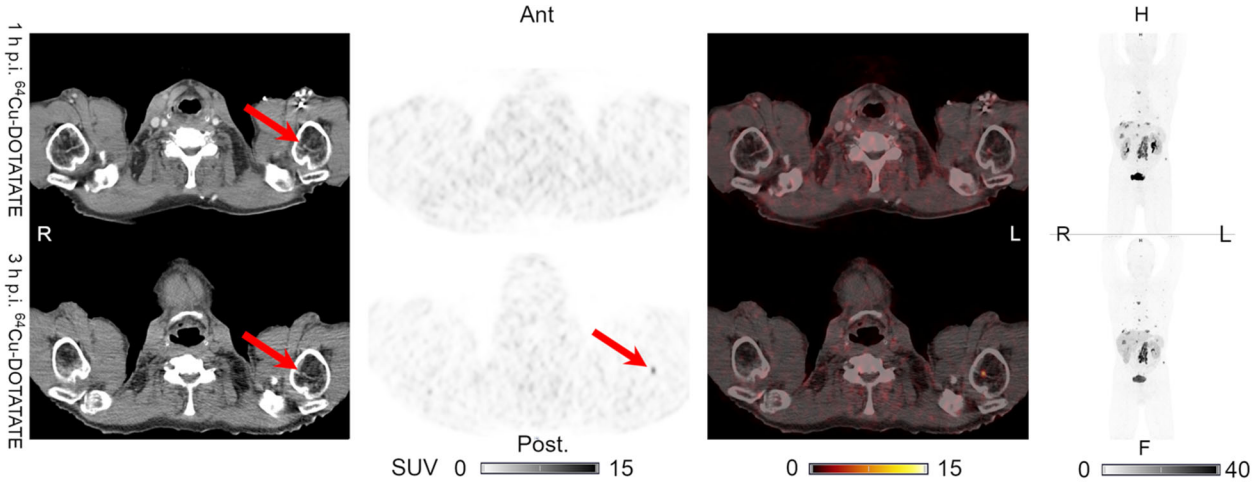

FIGURE 4 Patient 3: One additional liver lesion visible on 3h p.i. ^{64}Cu-DOTATATE PET (middle) but not on 1h p.i. ^{64}Cu-DOTATATE PET (top) without CT correlate. Discordant liver lesion visible on later 1h p.i. ^{68}Ga-DOTATOC-PET (46 months after the scan) with visible CT correlate (bottom). True positive. From left to right: CT, PET, fused PET/CT and MIP with corresponding SUV color bars below. Ant.: anterior, Post.: posterior, R: right, L: left, H: head, F: feet.

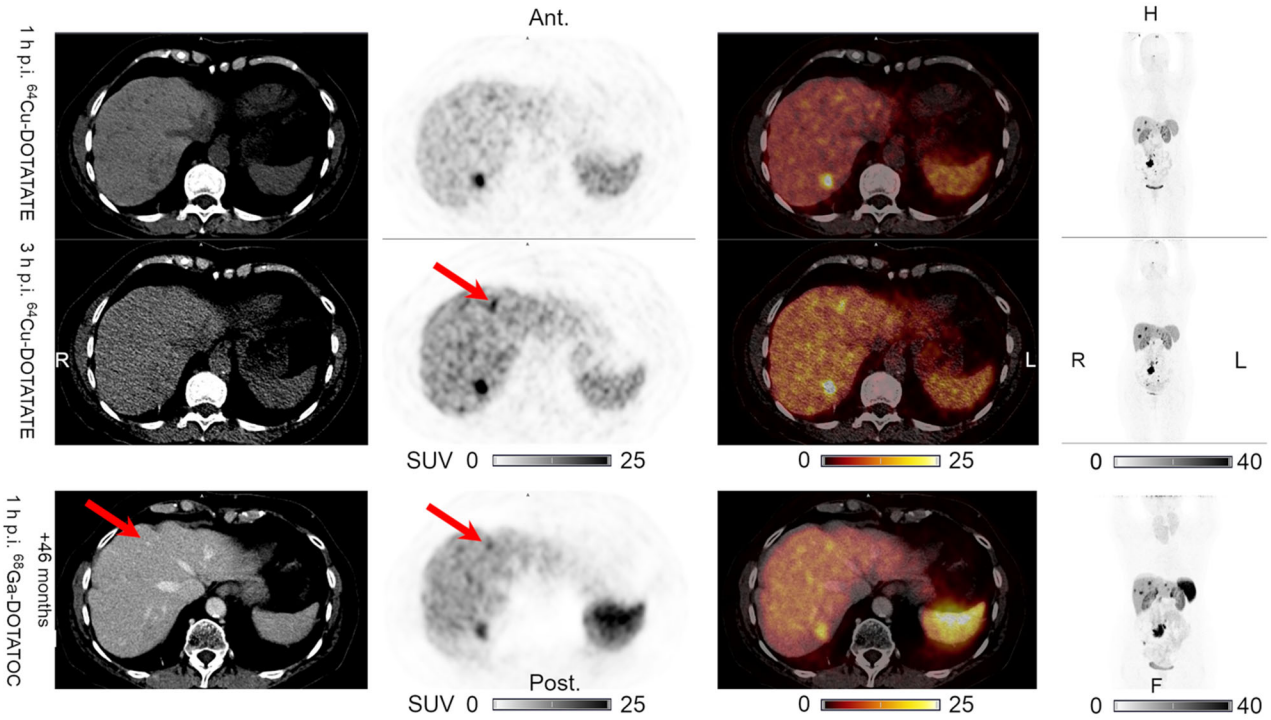

FIGURE 5 Patient 5: One additional liver lesion visible on 3h p.i. ^{64}Cu-DOTATATE PET (middle) but not on 1h p.i. ^{64}Cu-DOTATATE PET (top). No visible CT correlate. Discordant liver lesion visible on later 1h ^{68}Ga-DOTATOC-PET/CT (39 months after the scan) without visible CT correlate (bottom). True positive. From left to right: CT, PET, fused PET/CT and MIP with corresponding SUV color bars below. Ant: anterior, Post: posterior, R: right, L: left, H: head, F: feet.

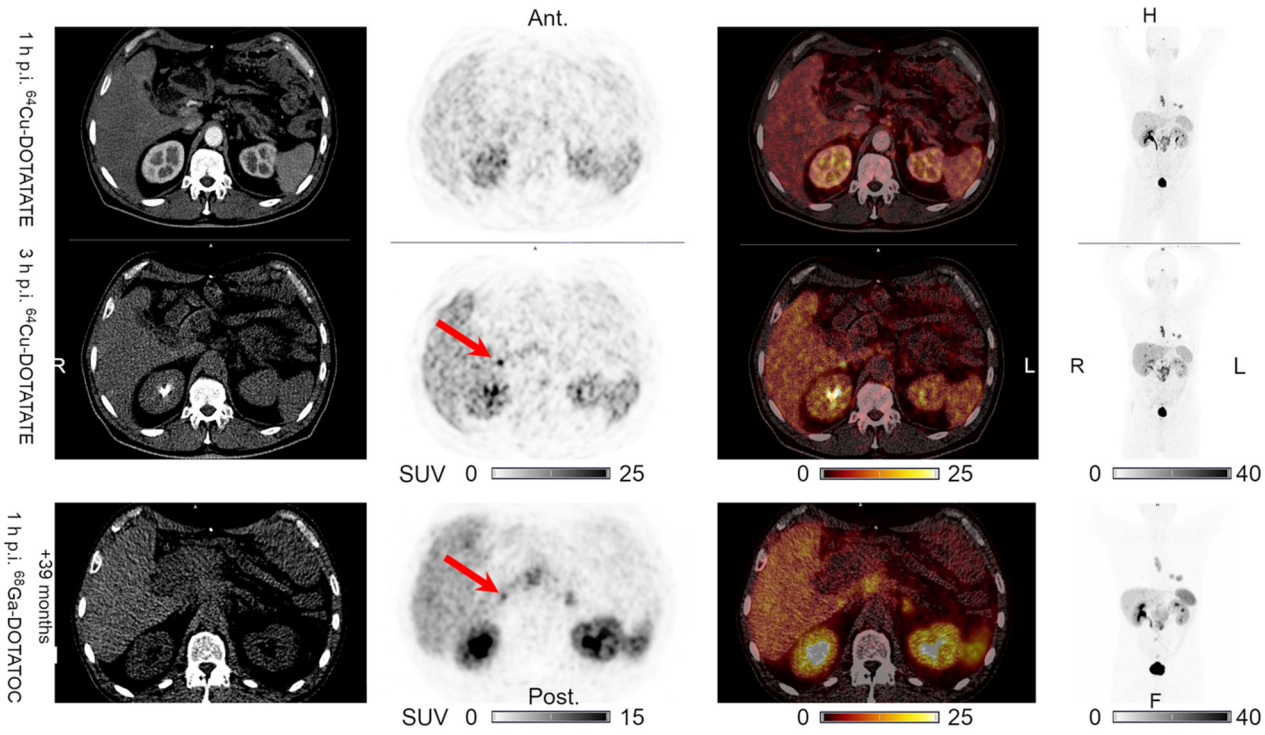

FIGURE 6 Patient 2: One additional bone lesion visible on the 1h p.i. ^{64}Cu-DOTATATE PET (top) but not 3h p.i. ^{64}Cu-DOTATATE PET without CT correlate (bottom). No later SSTR-PET available. No visible CT correlate on the latest CT-scan (8 months after the ^{64}Cu-DOTATATE PET/CT). False positive. From left to right: CT, ^{64}Cu-DOTATATE PET, fused ^{64}Cu-DOTATATE PET/CT and MIP with corresponding SUV color bars below. A: anterior, P: posterior, R: right, L: left, H: head, F: feet.

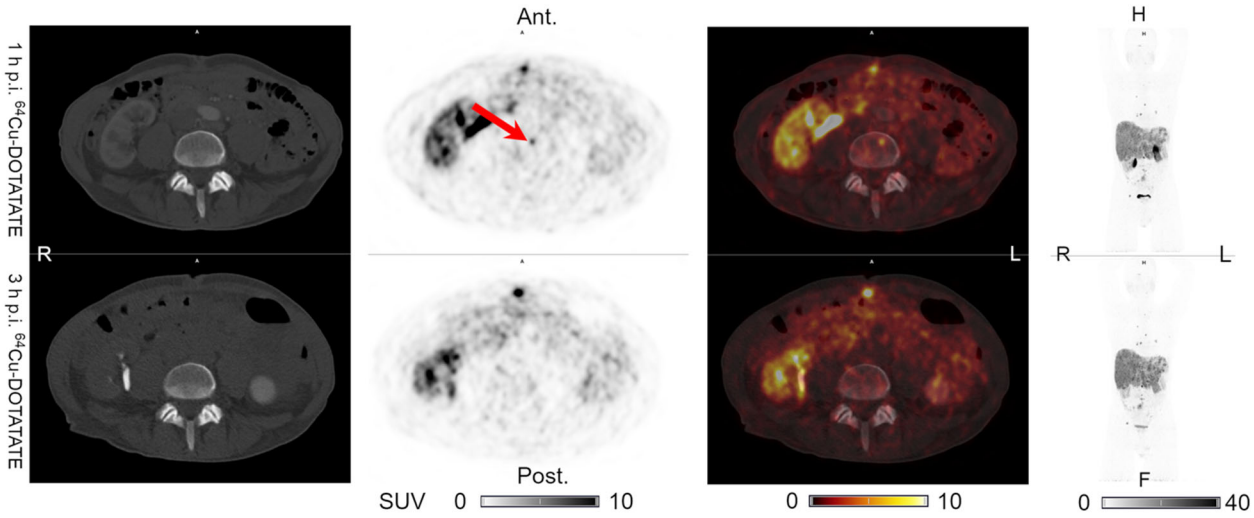

TABLE 1 Characteristics of 35 patients with neuroendocrine neoplasms examined on 1h and 3h p.i. ^{64}Cu-DOTATATE PET/CT.

	Total: 35 patients
Gender n (%)	
Male	21 (60%)
Female	14 (40 %)
Age	
Mean [minimum, maximum]	62 [40, 81]
Site of Primary Tumor n (%)	
Lung	3 (9%)
Gastrointestinal	13 (37%)
Pancreatic	5 (14%)
Other	2 (6%)
Unknown	12 (34%)
Functional Status n (%)	
Non-functioning	20 (57%)
Functioning (carcinoid syndrome)	15 (43%)
Grade n (%)	
Low-grade (G1)	8 (23%)
Intermediate grade (G2)	21 (60%)
High grade (G3)	2 (6%)
KI-67 proliferation index not available	4 (11%)
Primary Tumor Removed n (%)	
No	20 (57%)
Yes	15 (43%)
Previous treatments* n (%)	
Surgery	15 (43%)
Interferon α	19 (54%)
Somatostatin analogues	14 (40%)
Radio frequency Ablation (liver metastases)	3 (9%)
External radiation therapy	1 (3%)
Peptide receptor radionuclide therapy (PRRT)	12 (34%)

*Some patients received multiple treatments. Therefore, the total number of treatments exceeded the number of patients.

TABLE 2 Comparison of lesions per organ or region in 35 patients with neuroendocrine neoplasms

Organ/region	Concordant lesions	Only on 1h p.i. ^{64}Cu-DOTATATE PET	Only on 3h p.i. ^{64}Cu-DOTATATE PET	P†
Lung	14	0	0	-
Liver	298	0	2	0.98
Intestines	18	0	0	-
Pancreas	12	0	0	-
Intra-abdominal Carcinomatosis	7	0	0	-
Bone	326	1	1	1.00
Lymph nodes	114	0	1	0.98
Other*	33	0	0	-
Total	822	1	4	0.99

*Other locations: 22 soft tissue lesions, 5 heart lesions, 1 prostate, 1 adrenal, 1 stomach, 1 thyroid, 1 brain and 1 spleen lesion. †P values for tests for differences in the number of lesions with negative binominal regression per organ or region, and the total number of lesions between the 1h p.i. and 3h p.i. ^{64}Cu-DOTATATE PET.

TABLE 3 Discordant lesions per patient comparison in 35 patients with neuroendocrine neoplasms

ID	Concordant	Only on 1h p.i. ^{64}Cu-DOTATATE	Only on 3h p.i. ^{64}Cu-DOTATATE	Status	Months until follow-up	Modality	Discordant organ system
1	Liver (11)		LN (1)	TP	0*/9	CT/Cu	LN
2	Bone (15), LN (7), Lung (1), Carc (1), Liver (43)	Bone (1)		FP	8	CT	None
3	Liver (6), LN (8), Int (1)		Liver (1)	TP	46/46	Ga/CT	None
4	Bone (19), Spleen (1), Int (1), Adre (1), Heart (3), Liver (5)		Bone (1)	TP	0*	CT	None
5	Liver (2), LN (19) Heart (2), Int (1)		Liver (1)	TP	39	Ga	None

*Visible CT correlate on the ^{64}Cu-DOTATATE PET/CT. LN = Lymph nodes, Carc = intra-abdominal carcinomatosis, Adre = adrenal, Int = intestines, TP=true positive, FP = false positive, Ga = ^{68}Ga-DOTATOC PET, Cu = 1h p.i. ^{64}Cu-DOTATATE PET (follow-up scan).

TABLE 4 Lesion SUV_{max} in 35 patients with neuroendocrine neoplasms

		Lesion SUV_{max}†		
Organ / region	**n***	**1h p.i. ^{64}Cu-DOTATATE**	**3h p.i. ^{64}Cu-DOTATATE**	**P§**
Lung	5	17.9 [3.0; 32.9]	18.7 [5.3; 32.1]	1.00
Liver	22	45.7 [37.2; 54.3]	54.1 [44.3; 64.0]	<0.01
Intestines	12	64.4 [43.9; 84.8]	77.8 [52.3; 103.3]	0.19
Pancreas	8	79.0 [38.3; 119.6]	85.9 [35.9; 135.8]	1.00
Bone	12	44.2 [25.7; 62.7]	50.1 [29.7; 70.4]	0.46
Intra-abdominal carcinomatosis	4	23.0 [7.7; 38.3]	24.9 [9.0; 40.7]	1.00
Lymph nodes	18‡	40.9 [26.9; 54.9]	43.5 [29.1; 58.0]	0.76

*Number of patients with lesions. †Mean [95% CI]. ‡One additional lymph node lesion detected in one patient on the 3h p.i. ^{64}Cu-DOTATATE PET (n=19 on 3h p.i. PET). §P-values for paired T-tests adjusted for multiple comparisons with Bonferroni correction (N=7) and capped at 1.00.

TABLE 5 Normal tissue and organ SUV_{mean} in 35 patients with neuroendocrine neoplasms

		Normal organ or tissue SUV_{mean}†		
Organ / region	**n***	**1h p.i. ^{64}Cu-DOTATATE**	**3h p.i. ^{64}Cu-DOTATATE**	**P‡**
Lung	35	0.27 [0.23; 0.30]	0.15 [0.13; 0.17]	<0.01
Liver	32	4.0 [3.6; 4.4]	5.7 [5.2; 6.3]	<0.01
Intestines	35	2.6 [2.1; 3.1]	2.5 [2.0; 3.1]	1.00
Uncinate process of pancreas	31	3.2 [2.7; 3.6]	3.3 [2.7; 3.9]	1.00
Cauda of pancreas	32	3.1 [2.8: 3.5]	3.5 [3.2; 3.9]	0.38
Bone	35	0.76 [0.66; 0.85]	0.64 [0.56; 0.73]	<0.01
Muscle	35	0.63 [0.57; 0.69]	0.49 [0.44; 0.54]	<0.01
Spleen	35	8.9 [7.8; 10.0]	9.3 [8.2; 10.4]	0.12
Pituitary gland	35	12.9 [10.8; 14.9]	15.8 [13.4; 18.2]	<0.01
Adrenal gland	33	9.5 [8.0; 11.0]	9.9 [8.2; 11.6]	1.00

*Number of patients with evaluable normal organ or tissue. †Mean [95% CI]. ‡P-values for paired T-tests adjusted for multiple comparisons with Bonferroni correction (N=10) and capped at 1.00.

TABLE 6 Tumor to normal tissue/organ ratios (TTN) in 35 patients with neuroendocrine neoplasms

		TTN†		
Organ / region	**n***	**1h p.i. ^{64}Cu-DOTATATE**	**3h p.i. ^{64}Cu-DOTATATE**	**P§**
Lung	5	87.9 [30.2; 145.6]	160.9 [79.2; 242.6]	0.04
Liver	19	12.6 [10.2; 14.9]	11.0 [8.7; 13.4]	0.03
Intestines	12	24.2 [14.9; 33.4]	28.2 [16.5; 40.0]	0.73
Pancreas	6	42.4 [12.3; 72.5]	41.1 [8.7; 73.4]	1.00
Bone	12	103.0 [38.6; 167.4]	124.2 [57.1; 191.2]	0.07
Intra-abdominal Carcinomatosis	4	14.0 [3.0; 25.0]	22.5 [7.1; 38.0]	0.50
Lymph nodes	18‡	73.7 [43.0; 104.4]	94.0 [61.6; 126.4]	0.07

*Number of patients with lesions and evaluable normal tissue. †Mean [95% CI]. ‡One additional lymph node lesion detected in one patient on 3h p.i. ^{64}Cu-DOTATATE PET (n=19 on 3h p.i. PET). §P-values for paired T-tests adjusted for multiple comparisons with Bonferroni correction (N=7) and capped at 1.00.